Mechanical Design and Configuration of Penetrations for the Europa Clipper Avionics Vault Structure

Nicholas Keyawa
Jet Propulsion Laboratory,
California Institute of Technology
4800 Oak Grove Drive
Pasadena, CA 91109
Nicholas.R.Keyawa@jpl.nasa.gov

Ali Bahraman
SM IEEE
Bastion Technologies.
215 N. Marengo Ave
Pasadena, CA 91101
Ali.Bahraman@jpl.nasa.gov

William Hatch[3], Katherine Dang[4], Louis Giersch[5]
Jet Propulsion Laboratory,
California Institute of Technology
4800 Oak Grove Drive
Pasadena, CA 91109
[3]William.A.Hatch@jpl.nasa.gov
[4]Katherine.Dang@jpl.nasa.gov
[5]Louis.R.Giersch@jpl.nasa.gov

Abstract—**The main purpose of the Avionics Vault is to shield radiation sensitive electronics for the Europa Clipper Spacecraft. The vault is a box structure made out of aluminum panels. The panels are roughly 10 mm thick in order to shield the electronics from the orbital total ionizing radiation around Jupiter. The vault requires an electromagnetic interference (EMI) shielding effectiveness (SE) of at least 70 dB in order to mitigate EMI with the spacecraft radar receiver. Overall, the vault accommodates four main types of penetrations: receptacle connectors, pass-through cables, fluid lines, and vent holes. More than 150 cables penetrate the vault panels to connect to electronic boxes inside. Fluid pipes enter and exit the vault to transfer heat to the rest of the spacecraft. Vent holes provide a path for air to escape from the vault during launch. Several novel penetrations designs were created to meet EMI and radiation shielding requirements. Receptacle connectors interface to the vault panels using 1.3 mm thick Ta10W plates. Pass-through cables penetrate the vault using aluminum clamshells after being wrapped with Teflon cushion tape, Kapton tape, and copper tape. Vent hole penetrations consist of a copper mesh for EMI shielding and an aluminum radiation shield bracket to direct air out of the vault during launch. Fluid lines terminate at the vault wall using mechanical fittings that resemble a nut and bolt interface. In addition, most mechanical seams and penetrations utilize EMI gaskets to ensure proper EMI shielding. To reduce risk and confirm that the vault penetration designs were appropriate for EMI shielding, an EMI chamber at the Jet Propulsion Laboratory (JPL) was used to test a mock-up vault panel with multiple variations of all four main types of vault penetrations. This EMI SE test also incorporated different methods for bundling pass-through cables, and a comparison of flange mounted connectors versus jam nut connectors. A low noise preamplifier and a Rohde & Schwarz spectrum analyzer measured E-field levels transmitting through the mock-up vault panel. The results showed a shielding effectiveness of 77 dB for the mock-up vault panel, which exceeds the 70 dB target for Europa Clipper. Both the flange mounted connectors and jam nut connectors exhibited similar EMI SE results at the measured frequencies, and all variations of vault penetrations showed favorable EMI SE levels. Since the flight panels will be much larger and include many more penetrations, there will be testing of the flight vault to confirm its EMI SE is compliant with environmental requirements.**

TABLE OF CONTENTS

1. INTRODUCTION

The objectives of the Europa Clipper Spacecraft are to study Europa's ice shell, oceans, composition, and geology. In order to achieve these objectives, the spacecraft is equipped with nine instruments, as listed in Table 1.

Table 1: List of instruments on Europa Clipper

#	Instrument Title	Acronym
1	Europa Thermal Emission Imaging System	E-THEMIS
2	Mapping Imaging Spectrometer for Europa	MISE
3	Europa Ultraviolet Spectrograph	UVS
4	Europa Imaging System	EIS
5	Radar for Europa Assessment and Sounding: Ocean to Near-surface	REASON
6	Interior Characterization of Europa using Magnetometery	ICEMAG
7	Plasma Instrument for Magnetic Sounding	PIMS
8	Mass Spectrometer for Planetary Exploration	MASPEX
9	Surface Dust Mass Analyzer	SUDA

Seven of these instruments have electronic boxes that require protection from orbital radiation. In addition, the spacecraft has radiation monitors, power supplies, IMUs, star trackers, thermal pumps, and digital sun sensor electronic boxes that require protection from Jupiter's radiation environments. All of these electronic boxes mentioned above are shielded from Jupiter's radiation inside of a box structure known as the Avionics Vault. In total, there are about 26 electronic boxes inside of the vault, and more than 150 cables that need to penetrate the vault panels. Furthermore, the vault has fluid lines that gather heat from these electronic boxes, and penetrates the vault panels in order to distribute heat to the rest of the spacecraft. Lastly, four vent holes are in each corner of the vault in order to vent air during launch and cruise. The challenge in the design of the vault is accommodating these significant numbers of penetrations while maintaining radiation and EMI shielding effectiveness.

The configuration of the Avionics Vault is described in Section 2 of this paper. Section 3 goes over the radiation shielding requirements of the vault and Section 4 the EMI shielding requirements. The mechanical design of penetrations for connectors, pass-through cables, vent holes, and fluid lines are described in Sections 5, 6, 7, 8, respectively. Section 9 presents an overview of an EMI test of a mock-up vault panel. Section 10 provides a summary.

2. AVIONICS VAULT CONFIGURATION

The vault is roughly a 1.4m x 1.4m x 1m box structure composed of six aluminum panels, as shown in Figures 1 and 2. Reference names for the six panels of the vault are ±X (blue) panels (blue), ±Y (green) panels, +Z (yellow) panel, and –Z (pink) panel. Inside the vault, electronic boxes reside on the ±Y panels and ±Z panels.

The majority of cable penetrations are located on the ±X panels, with some on the +Z panel. Fluid lines exist on the ±Y panels and –Z panel. In addition, fluid lines penetrate through the –Z panel on the +X side of the vault. Vent holes are located on the bottom corners of the –Z panel. The +Z panel is designed to hinge open up to 180° using ground support equipment in order to allow access inside the vault during spacecraft integration. In addition, batteries, instrument sensor heads, and secondary structures reside on the external faces of the vault panels. The vault is bolted to

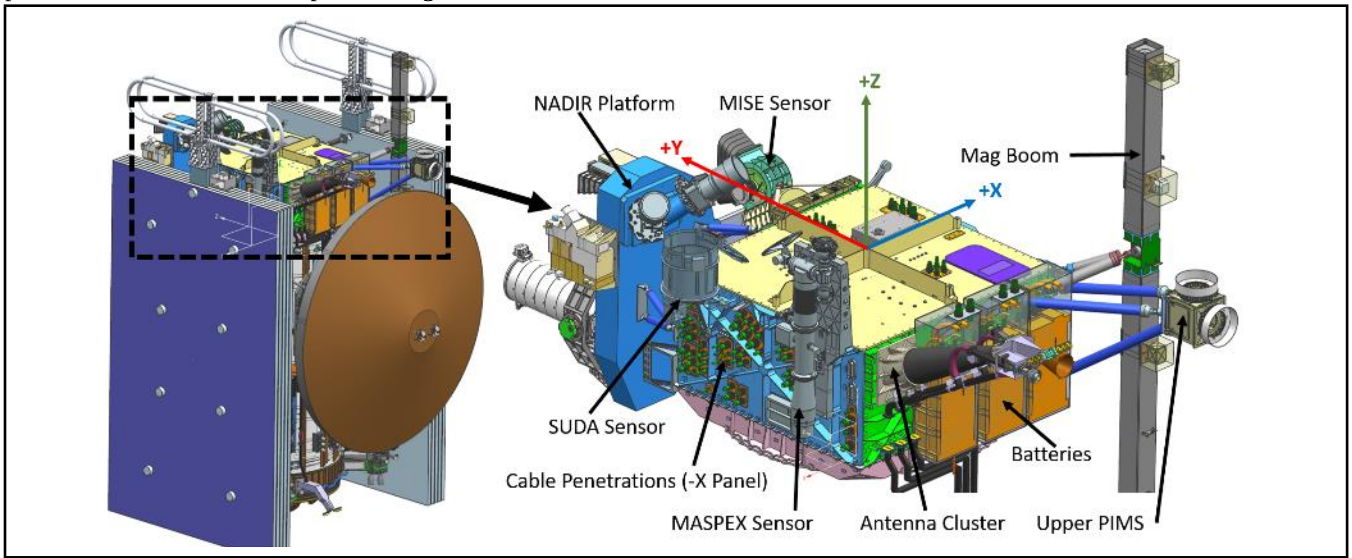

Figure 1. Configuration of the Avionics Vault structure on the Europa Clipper Spacecraft

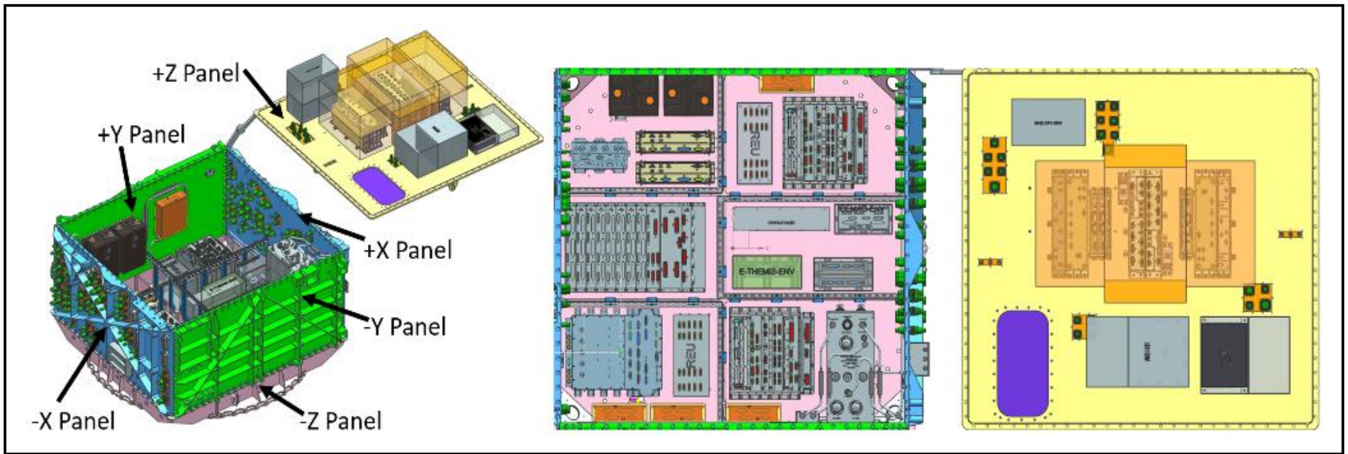

Figure 2. The Avionics Vault hinged open 180°, revealing the internal configuration of electronic boxes.

the Propulsion Module via the –Z panel, which is being developed by the Applied Physics Laboratory. Additional interfaces include the REASON Antenna Support Monopods on the ±X panels, the Antenna Cluster on the –Y panel, and the Magnetometer Boom Launch Restraints on the –Y/+X panels of the vault. The vault panels are Al 7075 due to its higher strength compared to other aluminum alloys and good thermal conductivity. In total, the six aluminum panels weight about 200kg.

3. Radiation Shielding

The main purpose of the Avionics Vault is to shield all sensitive electronics on the Europa Clipper spacecraft from the radiation environments around Jupiter. Inside the vault, the ionizing radiation dose rate is about 150 mrad(Si)/s, assuming a worst case total radiative dose of 3 Mrad around Jupiter, as specified in the Europa Environment Requirements Document (ERD). In order to meet this requirement, the vault needs to provide a radiation shielding effectiveness that is equivalent to 9.2 mm thick Al 7075. This means that the wall thickness of the Al 7075 vault panels need to be 9.2 mm thick, and Al 7075 mechanical joints that close the vault need to overlap by 9.2mm, as shown in Figure 3.

In addition to Al 7075, the vault has stainless steel alloys and tantalum alloys as radiation shields. A conservative approach to estimate the required radiation shielding thickness for these different metals (t_{new}) is to multiply the Al 7075 radiation shielding thickness by the ratio of the material densities, as shown below.

$$t_{new} = 9.2\left(\frac{\rho_{Al\,7075}}{\rho_{new}}\right) \quad (1)$$

In the equation above, ρ_{new} is the density of the new material, $\rho_{Al\ 7075}$ is the density of Al 7075. As noted above, this approach is conservative in that it does not account for the added bonus of high-Z materials, where the molecular structure provides a more mass efficient shield to radiation.

3. EMI Shielding

The Avionics Vault is required to achieve an EMI shielding effectiveness of at least 70 dB at the REASON radar frequencies of 9 MHz and 60 MHz when measured at 1 m from the vault panel. Since the vault consists of multiple panels and hundreds of penetrations, the resulting seams can significantly degrade the vault's EMI SE. Any metal-to-metal joint creates a seam, which can result in gaps for EMI signals to leak out. The vault design incorporates three techniques to minimize EMI signal leakage through seams: Spira-Shield EMI gaskets, Labyrinth L-configuration seams, and fastener spacing.

The Spira-Shield EMI gasket is a spiral wound metal made out of spring tempered beryllium copper[1]. The compression of this gasket in a seam provides up to 165 dB of EMI shielding. The vault utilizes two sizes of EMI gaskets. Vault panel-to-panel interfaces use a 0.125 inch diameter gasket, and penetration interfaces use a 0.094 inch diameter gasket, as shown in Figure 4. Since the gasket for vault panel-to-panel interfaces spans meters in length, the gasket dimeter is larger to allow for easier handling and installation.

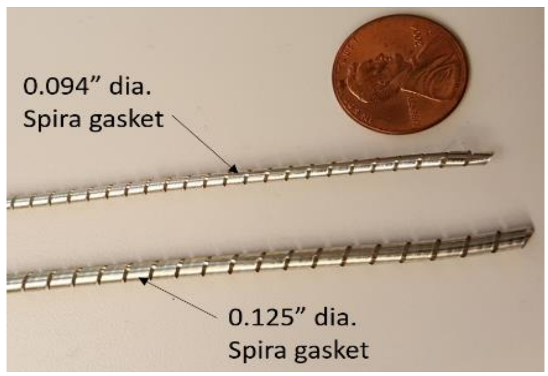

Figure 4. Two sizes of Spira-Shield EMI Gaskets used on the vault.

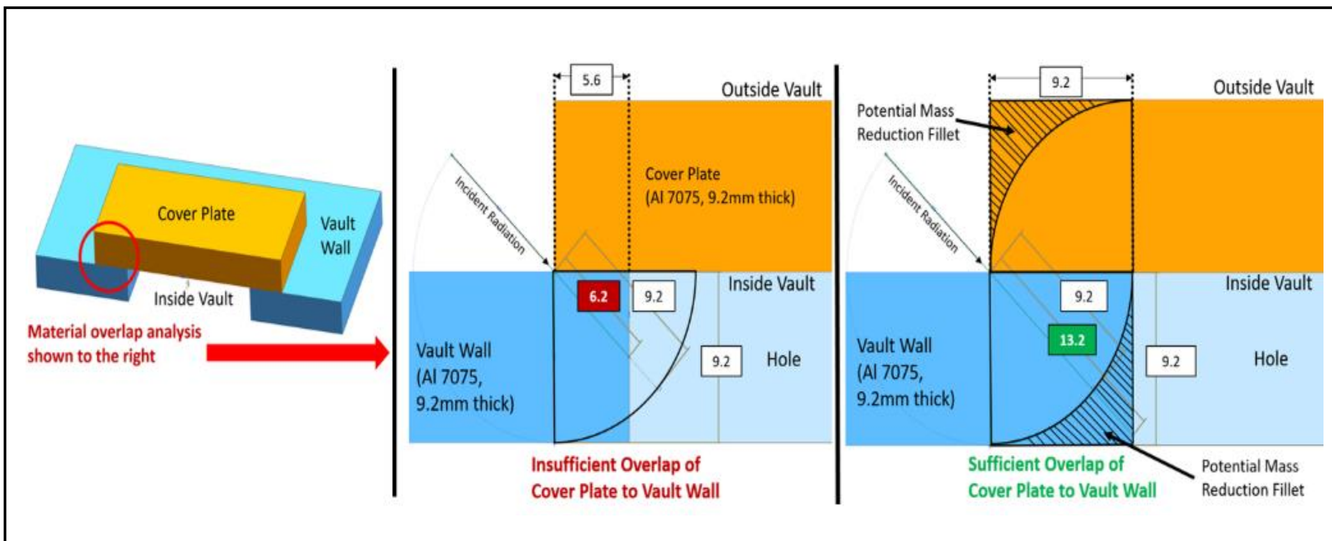

Figure 3. Illustration of required radiation shielding thickness for the vault walls and mechanical joints

All gaskets install into the vault panels via dovetail grooves, as shown in Figure 5. Dovetail grooves hold the spiral in place and facilitate easy field installation. Spira Manufacturing Corporation's website provides the recommended dovetail groove dimensions. Prototypes showed that the recommended dovetail groove dimensions were acceptable, except for the groove corner radius. The manufacturer recommends to use a groove corner radius of

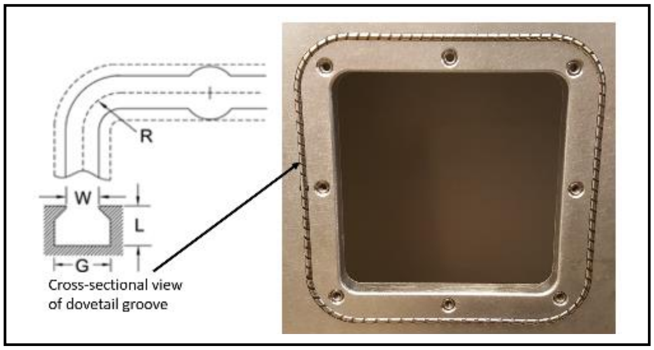

Figure 5. Installation of the Spira gasket into a dovetail grove around a clearance hole. The groove corner radius is 5 times the diameter of the gasket.

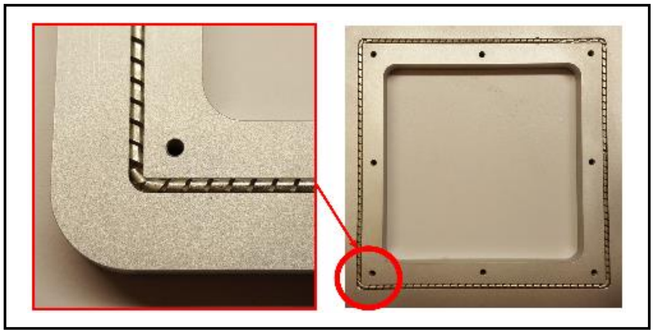

Figure 6. A damaged Spira gasket due to a groove corner radius of 1.5 times the diameter of the gasket.

1.5 times the diameter of the gasket or greater. However, testing showed that this minimum groove corner radius resulted in damaging the Spira gasket, as shown in Figure 6. The minimum groove corner radius was increased to about 5 times the diameter of the gasket to facilitate ease of installation and prevent damaging the gasket. Figures 5 and 6 provide a good comparison on how increasing the groove corner radius improved the overall installation of the gasket.

The Labyrinth L-configuration seams are illustrated in Figure 7. The Labyrinth L-configuration interferes with the direct line-of-sight access for electromagnetic radiation to leak out.

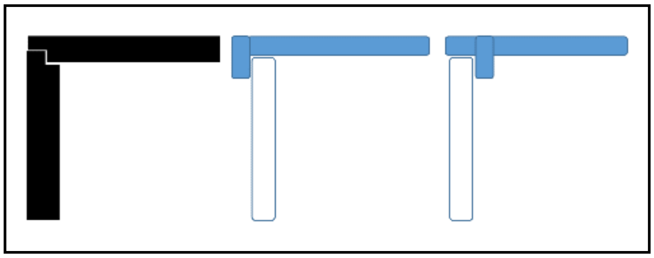

Figure 7. The Labyrinth L-configuration seams

The vault incorporates this seam configuration where Spira-Shield EMI gaskets are not possible.

All the panels of the vault and penetrations are held together using fasteners. The recommended fastener spacing to minimize gaps at each of these seams is no more than 50.8 mm (2 inches). This is shown in Figure 5, where there are miniature inserts for M3 size fasteners spaced at about 50mm apart around the perimeter of the vault clearance hole.

Additional design guidelines for EMI shielding are EMI grounding and vent hole conductive grids. For EMI grounding, the bonding impedance of a seam should not exceed 2.5 mΩ. If it does exceed 2.5 mΩ, a grounding strap is used. For venting, the vault has four vent holes that are 55 mm in diameter. The vent holes are sealed for EMI using a conductive grid, made out of copper wires, with holes less than 380 μm^2 (0.015 in^2). This is described in more detail in Section 7.

5. Receptacle Connector Penetrations

More than 150 cables need to penetrate the vault panels in order to connect to the electronic boxes inside. To accommodate this large quantity of cable penetrations, two panels of the vault have been dedicated to support these penetrations: the ±X panels. The vast majority of cables are penetrating the vault using rear mounted, flanged, MIL-DTL-38999 series II circular receptacle connectors, as shown in Figure 8. Other connectors that are penetrating the vault are rear mounted, flanged SMAs and micro-Ds. Having connectors at the vault panels allows for modularity of integration and provides a better EMI SE compared to pass-through cables.

Figure 8. A 24-35 rear mounted flanged, MIL-DTL-38999 series II circular connector. The flanged receptacle is on the left, and plug right.

In order for a rear mounted, receptacle connector to mate with its corresponding plug, the receptacle mounting plate cannot be more than 2-3 mm in thickness. In addition, it is advantageous in terms of access to have the ability to assemble the connectors outside of the vault. These guidelines advocate that the connectors are to mount to a connector plate that interfaces to the exterior vault panels. A promising material for these connector plates is Ta10W. Tantalum is a high-Z material that provides excellent shielding for total dose radiation at a thickness of about 1.3

mm, and the added tungsten provides significant strength and stiffness to the plates. Table 1 shows how Ta10W compares to other materials found on the vault structure. The Ta10W is just as strong and stiff as 316 stainless steel and has an acceptable electrical resistivity to ensure proper grounding of connectors to structure. In addition, the Ta10W has a much lower thermal conductivity compared to aluminum, which will help to minimize heat leaking away from thermal fluid lines and out through the connectors. Note that the radiation shield thickness of Al 7075 and Ta10W were determined from a spherical shell dose-depth curve. All other thicknesses were estimated using Equation 1. All materials properties were found from Metal Suppliers Online[2].

Table 1. Comparison of material properties

Metal	Radiation Shield Thickness (mm)	Density (g/cm^3)	Electrical Resistivity (Ω*cm)	Elastic Modulus (GPa)	Ultimate Tensile Strength (MPa)	Yield Strength (MPa)	Thermal Conductivity (W/m-K)
Al 6061-T6	9.6	2.7	4.00E-06	68.9	310	276	167
Al 7075-T73	9.2*	2.81	4.30E-06	72	505	435	155
Ta10W	1.3*	16.9	1.80E-05	205	550 - 620	482	54
316 SS	3.2	8	7.40E-05	193	579	290	16.2
Tungsten	1.3	19.3	5.50E-06	400	980	750	163

The overall integration flow of flanged receptacle connectors is described in Figure 9. From inside the vault, cable harnesses, with connector receptacles, pass through a large clearance hole in the ±X panels. From outside the vault, each of the flanged receptacle connectors fasten to a Ta10W plate via four flat fillister head #4-40 screws and nuts. Next, the Ta10W plate fastens to the vault panel via M3 socket head cap screws and inserts spaced every 50.8 mm or less, which compresses an EMI gasket around the Ta10W plate bolt pattern. The amount of added material to the Ta10W plate to compress the EMI gasket ensures that there is sufficient material overlap to close the vault clearance hole for radiation.

There are about 38 unique Ta10W connector plates to accommodate the more than 150 connectors on the ±X panels of the vault, as shown in Figure 10. Minimizing cable lengths and optimizing spacecraft integration access to the connectors drove the location and quantity of these connector plates. The size of the flanged connector, Spira-gasket, and M3 inserts in the vault panels drive the overall dimensions of the adapter plates, as shown in Figure 10.

6. PASS-THROUGH CABLE PENETRATIONS

There are some instances where cables cannot penetrate the vault panels via a connector. Adding connectors to a cable can cause impedance mis-match that impairs the quality of science data collected by an instrument. In addition, some instruments have high voltage cables that are incompatible with connectors. In these instances, cables need to pass-through the vault panels with no connector. Clamshells made out of Al 6061, as shown in Figure 11, provide a method that allows cables to pass-through the vault panels and close the penetration hole for EMI and radiation shielding.

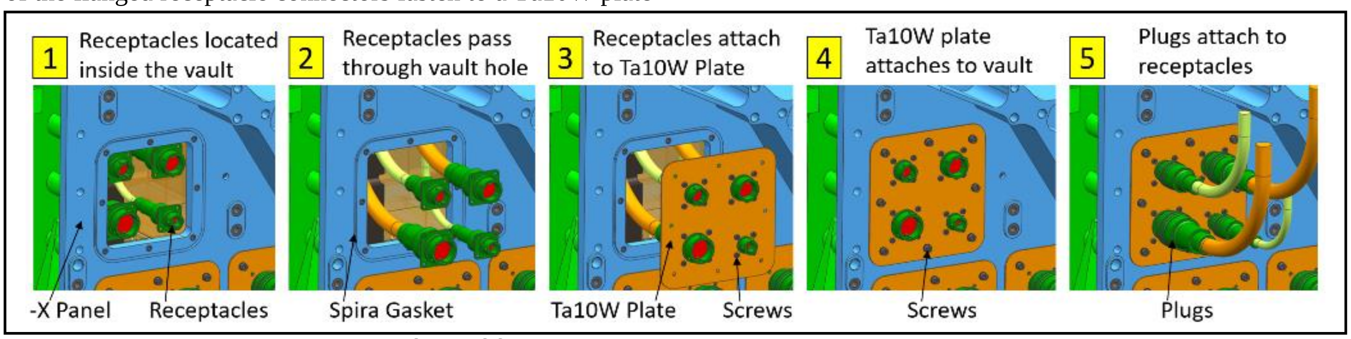

Figure 9. Integration flow of flanged, rear mounted circular connectors to the vault panels

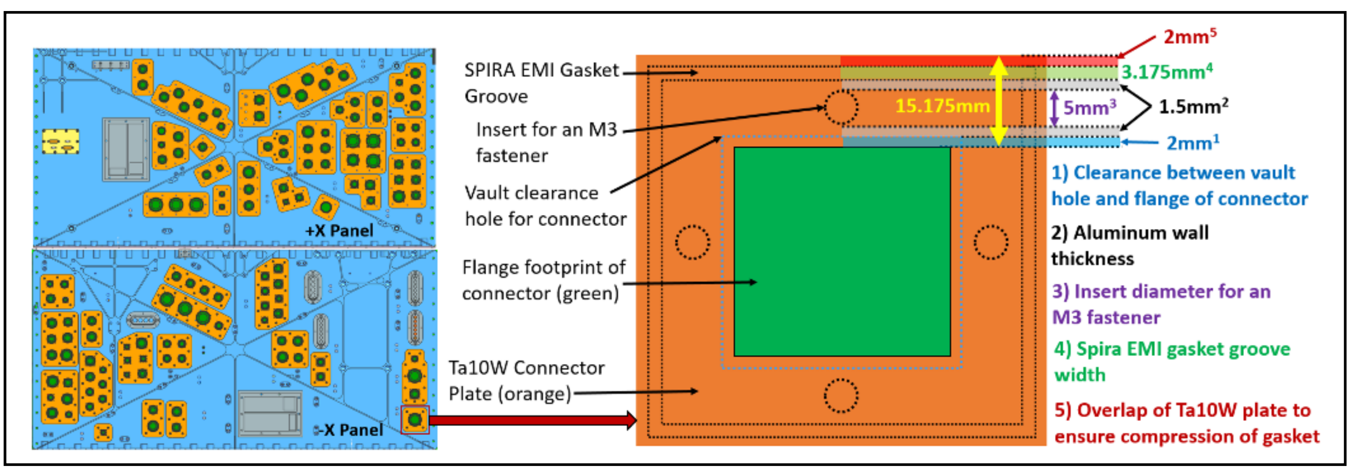

Figure 10. Arrangement and design of Ta10W connector plates on the X panels of the vault

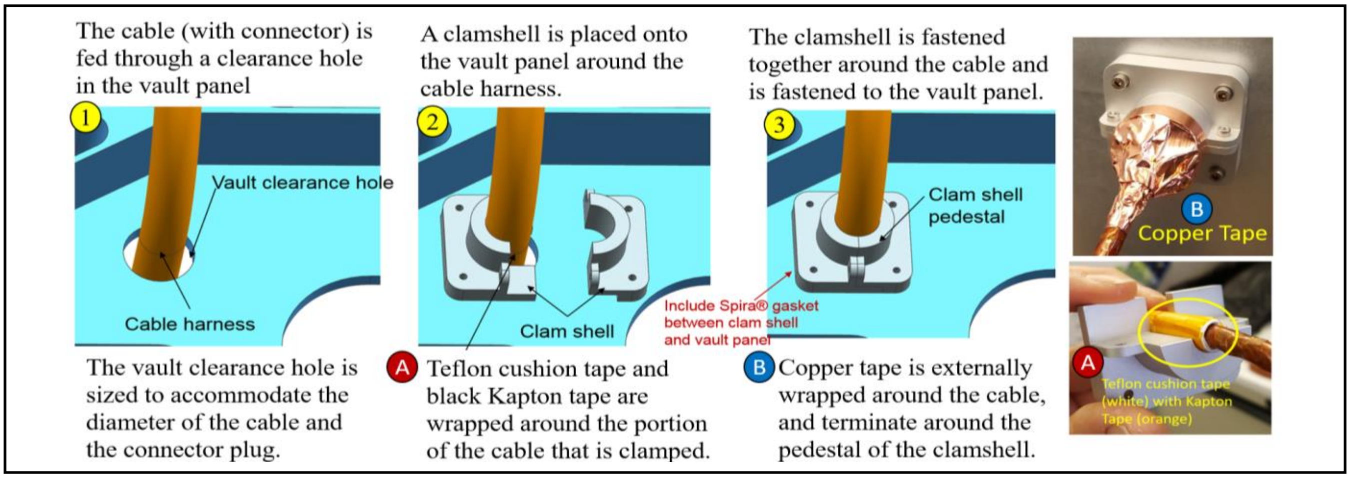

Figure 11. Illustration of how clamshells allow cables to pass-through the vault, and close penetration holes for EMI and radiation shielding.

First, the cable passes through a large clearance hole in the vault panel that is large enough for the cable's connector plug. Next, Teflon cushion tape and Kapton tape wrap around the portion of the cable that is clamped by the clamshell. The Teflon cushion tape and Kapton tape provide a compliant layer for safe compression around the cable, as shown in Figure 11. The two halves of the clamshell compress around the cable. Finally, the clamshell fastens to the vault panel, compressing an EMI gasket and closing the large clearance hole for EMI and radiation. In addition, the design of the clamshell incorporates a labyrinth L-seam to mitigate EMI signal leakages, as shown in Figure 12.

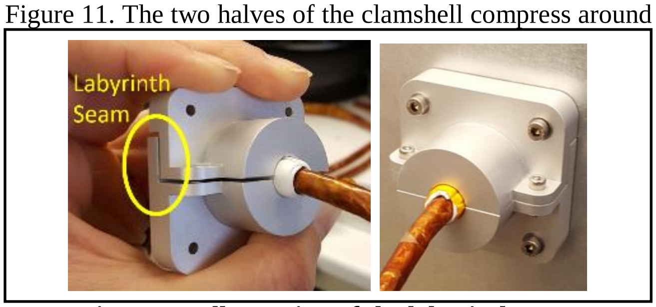

Figure 12. Illustration of the labyrinth seam

The clamping force around the Teflon cushion tape and Kapton tape does not provide an adequate seal for EMI shielding. In addition, the cable is not grounded to structure in this configuration. To mitigate this, the cable is wrapped with copper tape, which terminates around the pedestal of the clamshell, as shown in Figure 11(A) and 11(B).

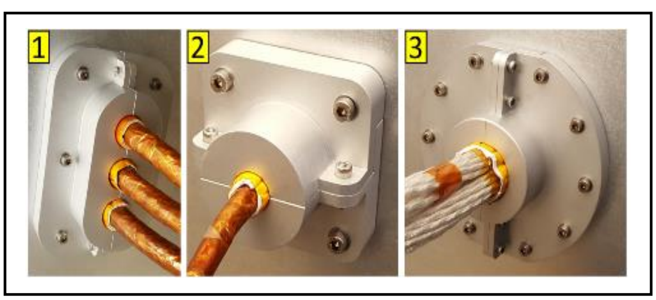

Figure 13. (1) A slotted clamshell, (2) single cable clamshell, and (3) cable bundle clamshell.

There are about 26 individual cables that pass-through the –X panel of the vault. Three different clamshells were developed to explore how to group these cables through a large clearance hole in the vault panel. These clamshell designs are shown in Figure 13. Of these three, the slotted clamshell was the most mass and space efficient approach to support multiple pass-through cables. In addition, the slotted clamshell provided more flexibility in tailoring the overwrap around each individual pass-through cable in order to ensure proper compression.

A more detailed design of the slotted clamshell is shown in Figure 14. The detailed slotted clamshell has a tapered pedestal to both reduce mass and to allow the copper tape more gradually wrap from cable to pedestal. A groove is also present for a metal band to wrap around and secure the copper tape to the pedestal. The pedestal has a taper such that the net thickness of the Al 6061 is 9.6 mm thick for any incident angle of radiation. There is an assumption that the cable itself provides adequate shielding for incident angles of radiation that follow directly down the axis of the cable. This is work to go to confirm via radiation modeling and analysis.

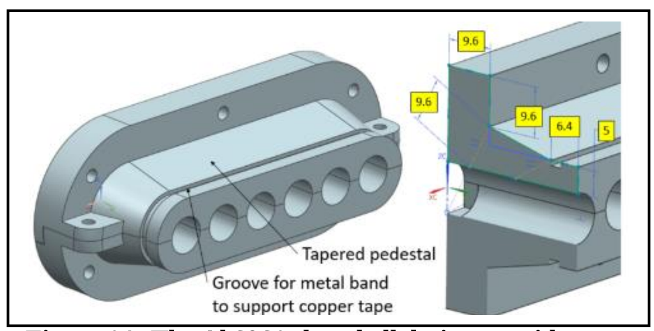

Figure 14. The Al 6061 clamshell design provides a net material thickness of 9.6mm for any incident angle of radiation.

7. VENT HOLES

During launch, the air inside the Avionics Vault needs to vent out in order to prevent the vault from becoming a pressurized vessel. A good rule of thumb for venting is to have the ratio of the void volume of the assembly and total area of the vent hole less than 50,800 mm. Assuming the vault is completely empty, the void volume of the vault is approximately 1.12 m^3. Assuming that there are four vent holes at each corner of the vault, the diameter of the vent holes would need to be about 84 mm to satisfy the rule of thumb for venting. In actuality, a significant amount of electronic boxes, support brackets, connectors, and cables reside inside the vault. This will drive cover can have significant mass since it needs to maintain the volumetric flow rate of the vent hole, have a radiation shielding thickness equivalent to 9.2 mm thick Al-7075, and generate a tortuous path for radiation so that there is no line-of-sight into the vault. To minimize mass of the radiation covers, the four vent holes exist at the corners of the vault and the radiation covers direct airflow towards the propulsion module, as shown in Figure 16. With the vent holes and radiation covers in these positons, the propulsion module provides shielding from radiation so that there is no line of sight into the vault, and air vents away from the multi-layer insulation (MLI) that blankets the entire spacecraft.

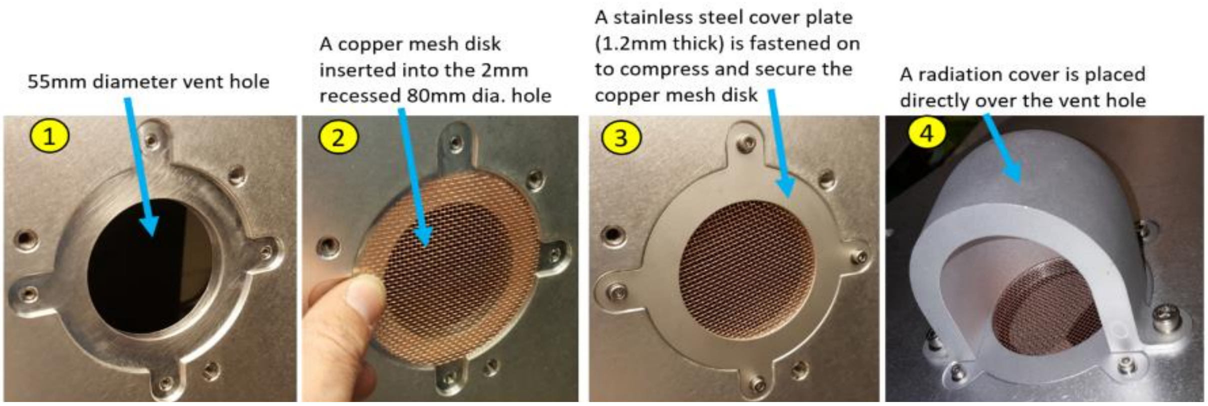

Figure 15. Components and assembly flow to close out vent holes for EMI and radiation shielding

the void volume down, and thus the required vent hole area down. In addition, the vault can probably handle higher levels of pressure during launch since the vault panels are significantly thicker and stronger than typical spacecraft chassis. With these factors in mind, the diameter of the four vent holes were set to 55 mm based on the space available at each of the four corners of the vault.

There are three components used to close a vent hole for EMI and radiation shielding, as shown in Figure 15. First, a copper mesh that has hole openings less than 380 μm^2 (0.015 in^2) covers over the vent hole. Next, a stainless steel plate fastens on to compress the copper mesh plate into the counterbore hole. The counterbore hole provides a more tortuous path for EMI signals. Finally, a radiation cover attaches over the stainless steel plate.

The design of the radiation cover is highly influenced by its relative location on the vault and spacecraft. The radiation

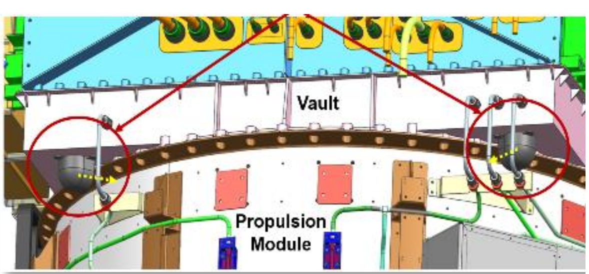

Figure 16. Location of vent holes on the vault

8. FLUID LINE PENETRATIONS

In total, four fluid lines penetrate the vault, as show in Figure 17. These four fluid lines are the propulsion module supply line, propulsion module return line, radiator supply line, and radiator return line. The fluid lines penetrate the +X side of the -Z panel wall, which is 9.2mm thick Al 7075.

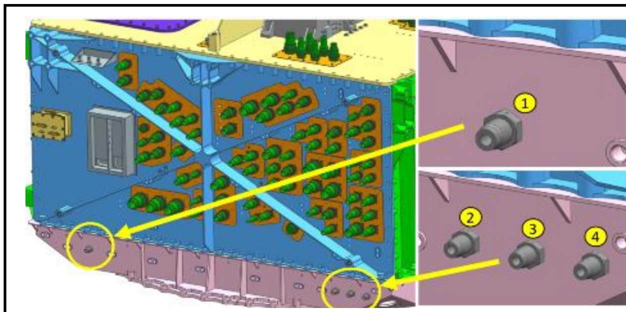

Figure 17. Location of fluid line penetrations on the vault. The fluid lines consist of a (1) propulsion module supply line, (2) radiator supply line, (3) radiator return line, and (4) propulsion module return line.

Fluid lines penetrate the vault via Omnisafe quick disconnect mechanical fittings, as shown in Figure 19. These mechanical fittings consist of a male nut, jam nut, female nut, torque eliminator, gasket, and gland. Of these components, only the jam nut and male nut are responsible for closing the vault clearance hole for EMI signals and radiation. As shown in Figure 18, a fluid line with a male nut slides through a

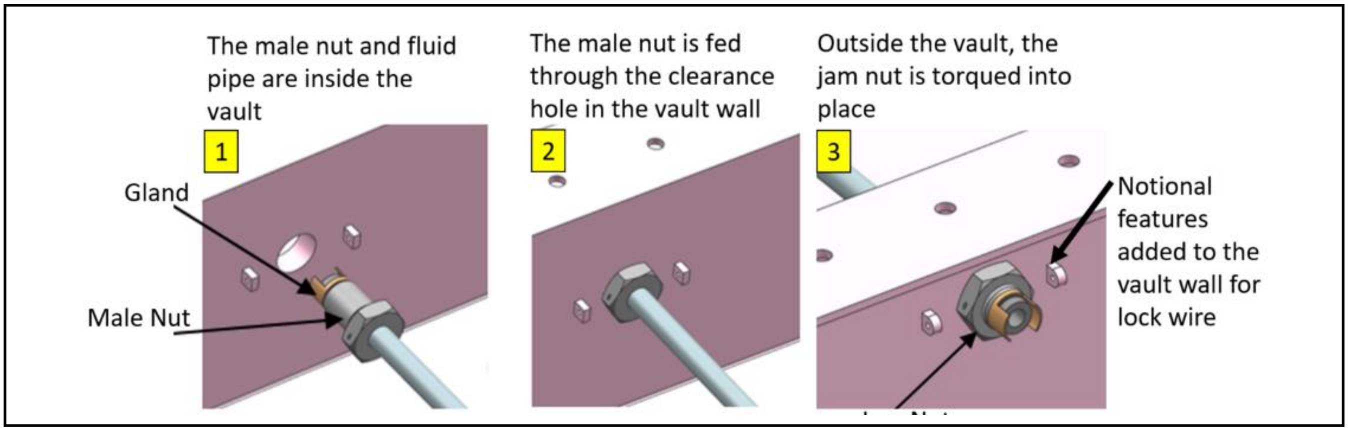

Figure 18. Integration of a fluid line mechanical fitting onto the –Z panel wall

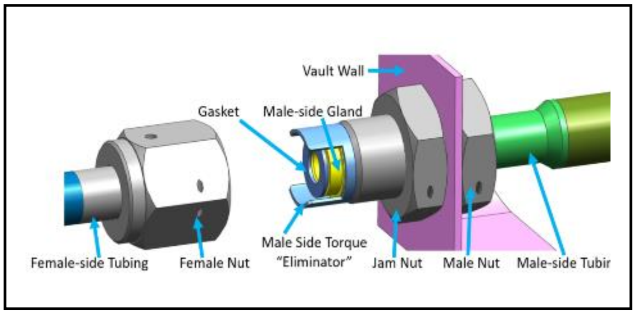

Figure 19. Components of an Omnisafe mechanical fitting. Vault wall shown is not to scale.

clearance hole in the vault panel. Next, a jam nut torques onto the male nut threads, which secures the fluid line to the vault panel. This method of securing the fluid line to the vault panel inadvertently seals the vault clearance hole for both EMI signals and radiation by creating a torturous path. In essence, this overall assembly is very similar to nut a bolt fastener assembly.

9. MOCK-UP VAULT PANEL EMI TEST

An EMI test was performed in the JPL EMC Lab in March 2018 in order to assess the EMI SE of the Europa Clipper Avionics Vault penetrations. The Vault must meet an EMI SE level of at least 70 dB as specified in the Europa ERD. This SE level is critical for ensuring the radiated emissions generated inside the vault will not cause interference with the REASON radar frequency (RF) subsystem in flight. The purpose of the EMI test was to reduce risk by confirming the panel design and construction were appropriate for EMI shielding.

Test Article: Mock-up Vault Panel

The test article, referred to as the mock-up vault panel, was a scaled down version of the vault X panels with dimensions of 28" x 28" x 0.4", as shown in Figures 20 and 21.The penetrations on the mock-up vault panel are described in Table 2. Spira EMI gaskets were used behind component numbers 1 thru 6.

Table 2. List of penetrations for the mock-up vault panel

#	Description of Penetration
1	A large connector adapter plate that consists of 6 circular connectors (flanged receptacles) mounted to a 1.3 mm thick Ta10W plate. The Ta10W and compresses an EMI gasket. Copper tape is used to cover any exposed wires or pins.
2	A small connector adapter plate that consists of 2 circular connectors (jam-nuts) mounted to a 1.3 mm thick Ta10W plate. The Ta10W and compresses an EMI gasket. Copper tape is used to cover any exposed wires or pins.
3	A clamshell for a ~10 mm in diameter single cable that penetrates the vault via a circular through hole. The cable is wrapped with Teflon cushion tape, Kapton tape, and copper tape that terminates around the pedestal of the clamshell. The clamshell compresses an EMI gasket.
4	A clamshell for multiple cables bundled together through a circular through hole. Wrapping is the same as the single cable clamshell (#3). The clamshell compresses an EMI gasket.
5	A clamshell for multiple cables that penetrate the vault via a slotted hole. Wrapping is the same as the single cable clamshell (#3). The clamshell compresses an EMI gasket.
6	A generic cover plate that acts as an access panel on the vault. The cover plate compresses an EMI gasket.
7	A torturous labyrinth path seam interface with no EMI gasket.
8	A 3/8" size nut and bolt that represents a single fluid line mechanical fitting.
9	A vent hole with copper mesh compressed under a cover plate, and a radiation cover.

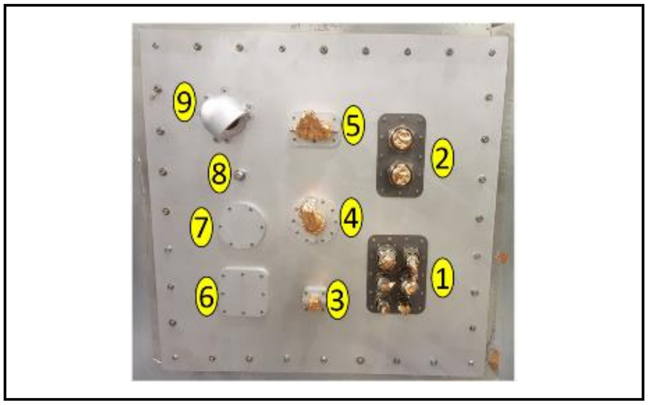

Figure 20. The mock-up vault panel installed on the EMI test chamber wall (control room side). Note that all exposed nodes are covered in copper tape.

Figure 21. The mock-up vault panel installed on the EMI test chamber wall (interior of chamber). Note that no copper tape was used on the penetrations.

Test Setup and Baseline Testing

A baseline test was performed, using the setup shown in Figure 22, to calibrate E-field versus signal generator (SG) drive power level.

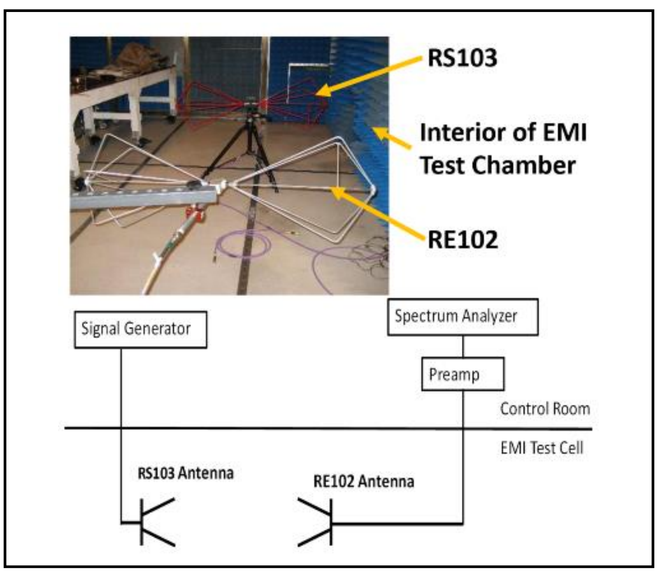

Figure 22. Baseline test setup schematic and physical test setup in the EMI chamber

The test setup and the spectrum analyzer settings were in accordance with the guidelines in MIL-STD-461F. The EMC32 test software was used to acquire the test data from the spectrum analyzer. The antenna spacing was 2 m apart, and the signal generator power setting was at -5 dBm. The results of the baseline test are shown in Appendix Figure A1.

Another baseline test was performed in order to understand how the size of the test chamber opening affects the E-field. As shown in Figure 23, the mock-up vault panel on the test chamber wall was removed and the RS103 antenna was placed at 1 meter from the opening inside the test chamber. The RE102 antenna was placed outside the test chamber at 1 meter from the test chamber opening. The RE102 test signal was measured via the Sonoma preamp and the Rohde & Schwarz spectrum analyzer. The results are shown in Appendix Figure A2 with the SG power increased to +10 dBm. Note that this level is 15 dB higher in the initial baseline test shown in Figure A1. If the data in Figure A2 are normalized to SG level of –5 dBm, the measurement would be 15 dB lower at 66 dBμV/m.

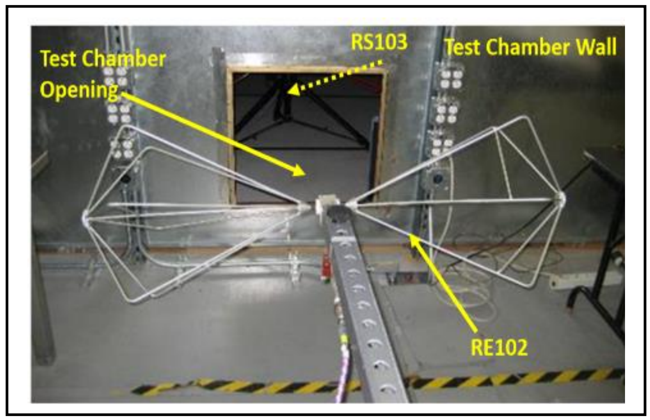

Figure 23. Second baseline test setup.

In other words, the square opening in the test chamber wall resulted in about 22 dB reduction in the E-field level relative to the antenna-to-antenna setup inside the test chamber. Part of this reduction is attributed to the size of the biconical antenna, which is larger than the size of the opening. Consequently, a mini-bicon RE102 antenna was used in later tests.

Baseline Shielding Measurement

The RS103 test antenna and the RE102 biconical antenna were set up to measure shielding response of the Engineering panel at 60 MHz, which is the VHF – band center frequency of the REASON RF subsystem. Figure 24 shows the test setup. Appendix Figure A3 shows the measured data on the spectrum analyzer. With SG at +10 dBm, the measured RE102 E-field was 17 dBμV/m. At SG at –5dBm, the measurement would be 2 dBμV/m. This compares well with the data in Figure A1 at 88 dBμV/m, with SG power at – 5 dBm. The resulting reduction in signal due to Test Article setup shielding is:

$$SE = 88 - [17 - 10 - (-5)] = 76 \text{ dB} \qquad (2)$$

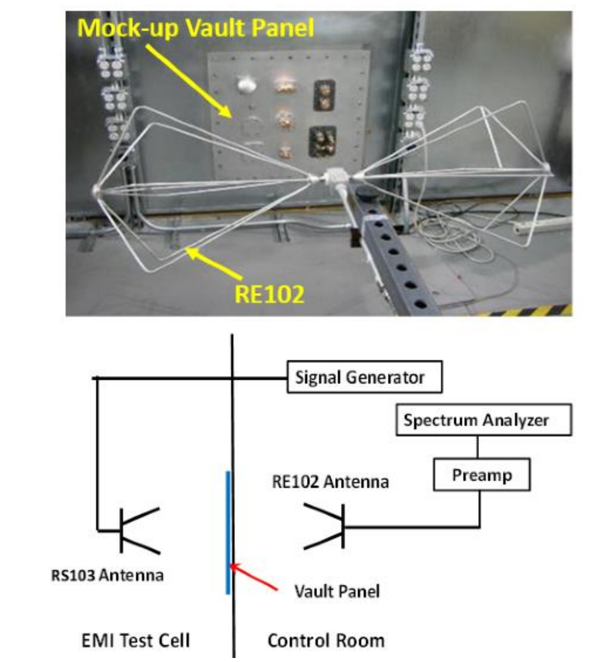

Figure 24. Baseline shielding measurement setup

Note that Figure A1 was for the antenna-to-antenna measurement in the test chamber at 2 m spacing between antennas. The antenna-to-antenna spacing for Figure 24 was also 2 m, but with the mock-up test panel installed in between. However, the biconical antenna is bigger than the width of the mock-up vault panel in Figure 23. Therefore, this setup over-states the shielding response. Hence, a mini-biconical antenna was used subsequently.

Shielding Test Using the Mini Biconical Antenna

The RE102 biconical antenna was replaced with a mini-bicon antenna, as shown in Figure 25. The test was repeated with SG power set at +15 dBm. The results are shown in Appendix Figure A4, with peak E-field at 10.65 dBµV/m.

Figure 25. Repeat of the baseline shielding measurement setup using the mini-bicon antenna

However, EMC32 uses the standard biconical Antenna Factor (AF) of 8.8 dB/m for calculating the E-field. The mini-bicon AF is 27 dB/m at 60 MHz per the antenna manual. Therefore, the EMC32 data must be corrected for the AF. The E-field is calculated from the SA reading as follows:

$$E\ (\mathrm{dB\mu V/m}) = V\ (\mathrm{dB\mu V}) + AF\ (\mathrm{dB/m}) \quad (3)$$

Therefore, with the Antenna Factor (ΔAF) correction,

$$\Delta AF = 27 - 9 = 18\ \mathrm{dBm} \quad (4)$$

the actual E-field was:

$$E = 10.65 + 18 = 28.65\ \mathrm{dB\mu V/m} \quad (5)$$

At – 5 dBm, the E-field would be 28.65 – [15 – (–5)] = 8.65 dBµV/m. From Test 1 results, the panel SE is:

$$SE = 87.6 - 8.6 = 79\ \mathrm{dB} \quad (6)$$

The mini-bicon antenna was moved inside the test chamber, as shown in Figure 26, to obtain baseline reference data with the mini-bicon for comparison with the test shown in Figure 25. The mini-Bicon antenna was placed at 1 meter from the RS103 Biconical antenna, which was driven at 15 dBm. Appendix Figure A5 shows the test data.

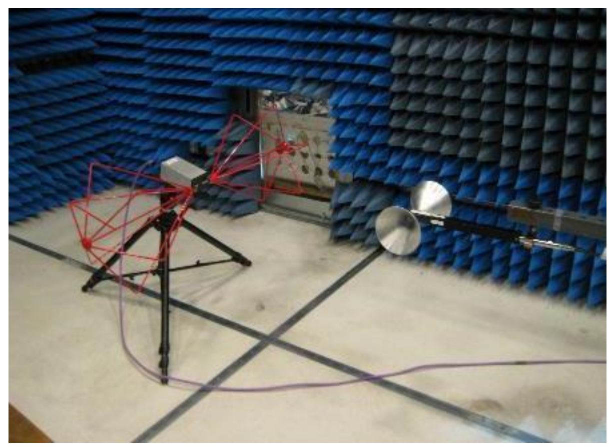

Figure 26. Repeat of the baseline calibration with the mini-bicon antenna

The E-field at 1 m was

$$E = 94.2 + 18 = 112.2\ \mathrm{dB\mu V/m} \quad (7)$$

From Equations (5) and (7), the SE result is

$$\mathbf{SE = 112.2 - 28.6 - 6 = 77\ dB} \quad \mathbf{(8)}$$

A correction of 6 dB is applied above since the data in Figure A5 are measured at 1 m, but Figure A3 measurement was at 2 m distance between transmit and receive antennas. The above result compares very favorably with 79 dB in Equation (6). The above results indicate the Vault engineering panel exceeded the SE requirement of 70 dB by at least 7 dB.

EMI Test Verification – Vent Hole

The vent hole EMI shielding copper mesh was foiled with EMI tape to assess its impact, as shown in Figure 27. The test setup in Figure 25 was repeated and measured data showed 9.975 dBµV/m at about 60 MHz. Comparing this to the data shown in Figure A4, the difference is only 0.7 dBµV/m. This indicates that the copper mesh on the vent hole achieves a high shielding effectiveness.

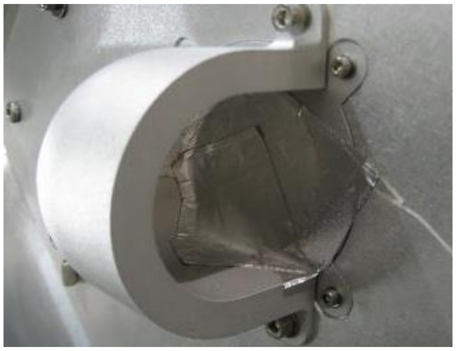

Figure 27. EMI tape placed over the vent hole in order to assess the EMI SE of the copper mesh

EMI Test Verification – Jam Nut versus Flanged Receptacle

An EMI test was performed to assess the relative shielding performance of the jam-nut connector and the flanged receptacle. The hypothesis is that the jam-nut connector provides a much more torturous path for EMI signals, and thus has a better EMI SE compared to the flanged receptacle connector.

To evaluate this hypothesis, all penetrations on the mock-up vault panel were shielded with aluminum foil except the connector of interest. Figure 28 shows all penetrations foiled except the jam-nut connector plate. The EMC32 measurement for this configuration at 59.95 MHz was 11.68 dBµV/m.

Figure 28. Configuration with all penetrations foiled except the jam-nut connector plate

Figure 29 shows all penetrations were foiled except the flanged connector plate. The EMC32 measurement for this configuration at 59.95 MHz was 11.72 dBµV/m.

The results for both the jam-nut and flanged receptacle connectors are essentially the same, indicating the two connectors have similar shielding. However, the flanged receptacle connectors had short cables connected on the interior of the test chamber, whereas the jam-nuts had no cables at all. These short cables might have provided improved shielding through the connector aperture.

Figure 29. Configuration with all penetrations foiled except the flanged receptacle connector plate

EMI Test Verification – Sniffing Probe the Seams

A near field probe was used to probe the seams of the penetrations on the mock-up vault panel to assess EMI leakage, as shown in Figure 30. The RS103 antenna was driven inside the test chamber and the probe was used at a selected seam to measure leakage. The signal generator power was increased to 20 dBm to provide more signal, and the probe output was connected to the Sonoma preamp, with its output routed to the spectrum analyzer set up for scans measuring dBµV. This configuration enabled measurement of very low signal levels.

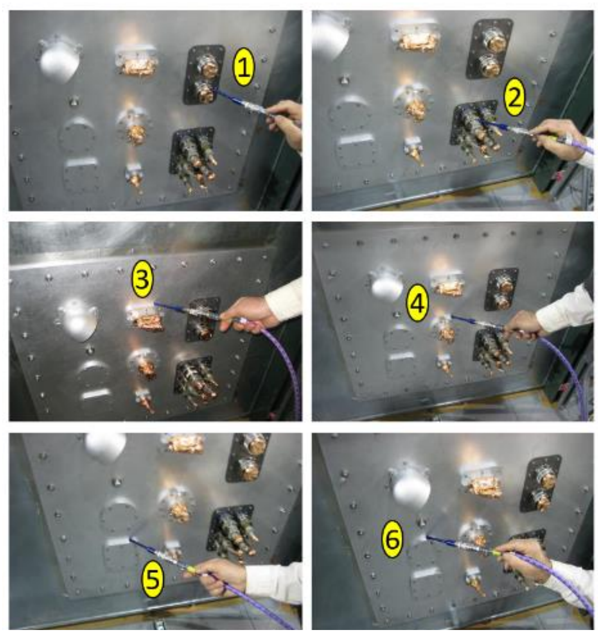

Figure 30. Location of sniffing probe for each penetration of interest

The test results showed very low leakage levels, consistent with the SE results reported above. Table 3 provides a summary of measurements, and the respective test setups are shown in Figure 30.

Table 3. Near Field Probe Measurements

#	Signal (dBμV)
1	5.6
2	7.8
3	8
4	8.1
5	8.1
6	7.5

Note that all thru-hole cables were foiled with EMI copper tape all the way to the clamshell pedestal. However, to assess the EMI SE of copper tape, the copper tape was removed from the clamshell as shown in Figure 31. The leakage increased from 8.1 dBμV to 39.8 dBμV. This illustrates the effectiveness of EMI tapes in closing leakage paths.

Figure 31. Sniff probe being used on a clamshell penetration with no copper tape.

10. SUMMARY

The Avionics Vault is a box structure that houses radiation sensitive electronics for the Europa Clipper Spacecraft. In order to provide the required radiation environment inside the vault, the panels are 9.2 mm thick Al 7075. All seams and additional materials used to close the vault for radiation need to provide a radiation shielding effectiveness equivalent to 9.2 mm thick Al 7075. The vault is also required to achieve an EMI SE of at least 70 dB at the REASON radar frequencies of 9 MHz and 60 MHz when measured at 1m from the vault panel. This is achieved using Spira-Shield EMI gaskets, Labyrinth L-configuration seams, and less than 2inch fastener spacing.

In total, there are four main types of penetrations on the vault: receptacle connectors, pass-through cables, fluid lines, and vent holes. Receptacle connectors are mounted to 1.3 mm thick Ta10W plate, which are sized to accommodate a Spira-Shield gasket. Pass-through cables penetrate the vault via slotted clamshells. Clamshells use Teflon cushion tape and Kapton tape for compression compliance around the cable and copper tape to close out for EMI signals. Vent holes have a copper mesh shield for EMI signals, and radiation shield that directs air away from the MLI around the spacecraft. Fluid pipes penetrate the vault using Omnisafe mechanical fittings, which creates a tortuous path for radiation and EMI signals.

To confirm that these novel penetrations provided adequate EMI shielding, an EMI test was performed at JPL on a mock-up vault panel. A low noise preamplifier and a Rhode & Schwartz spectrum analyzer measured E-field levels transmitting through the mock-up vault panel. The results showed a shielding effectiveness of 77 dB for the mock-up vault panel, which exceeds the 70 dB target for Europa Clipper. In addition, the flange mounted connectors and jam nut connectors exhibited similar EMI SE results. The EMI test verified the shielding effectiveness of the copper mesh and copper tape for vent holes and clamshell penetrations, respectively. Since the flight panels will be much larger and include many more penetrations, there will be testing of the flight vault to confirm its EMI SE is compliant with environmental requirements.

APPENDIX

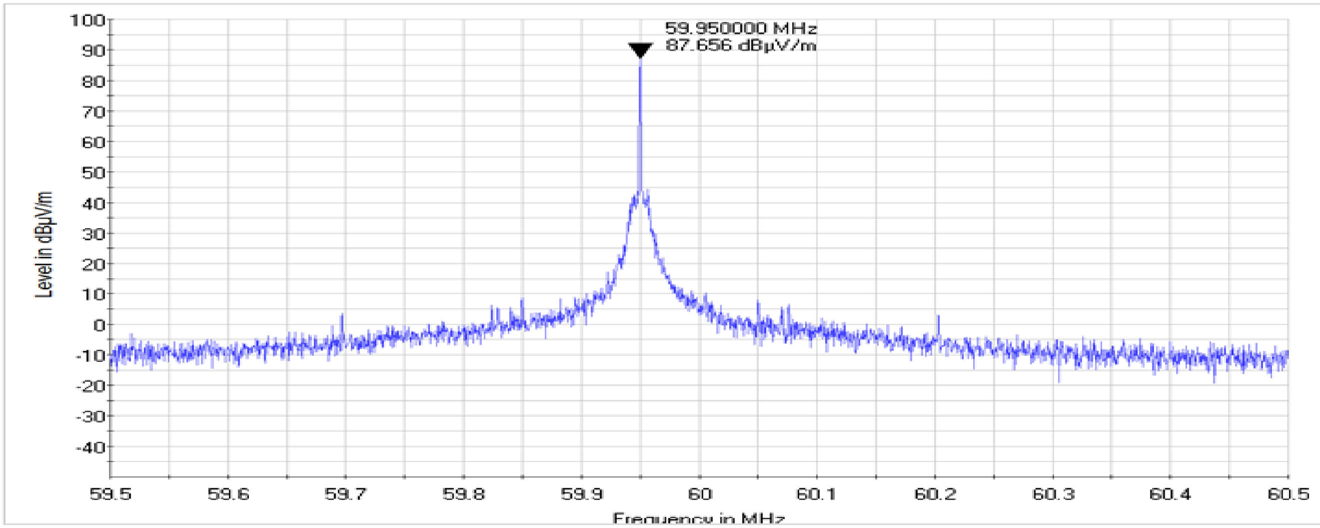

Figure A1. Test data for setup shown in Figure 22.

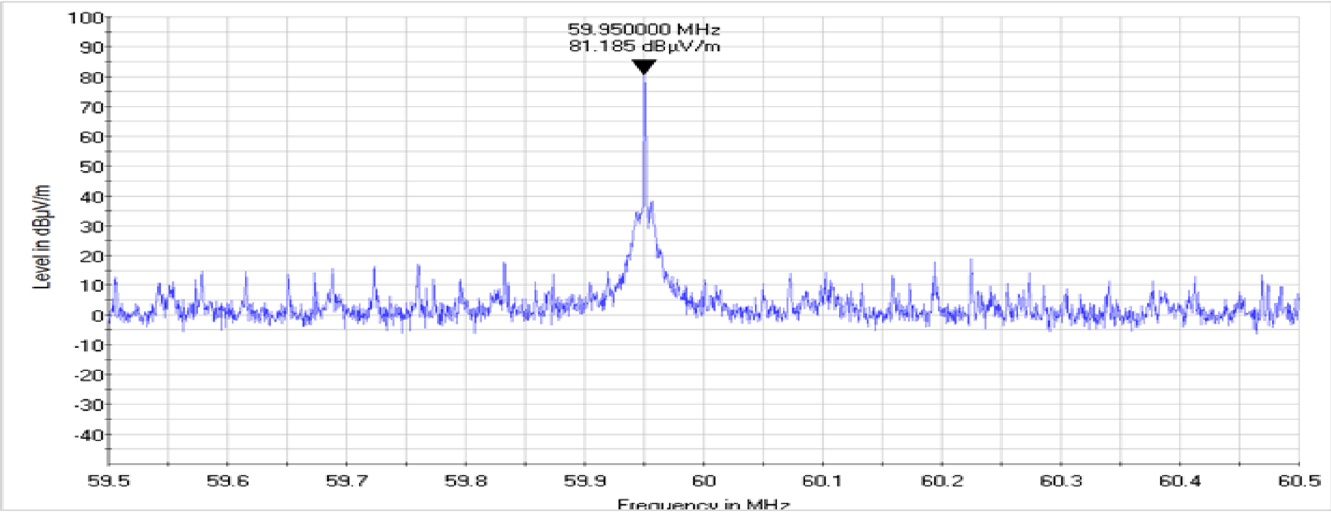

Figure A2. Test data for setup shown in Figure 23.

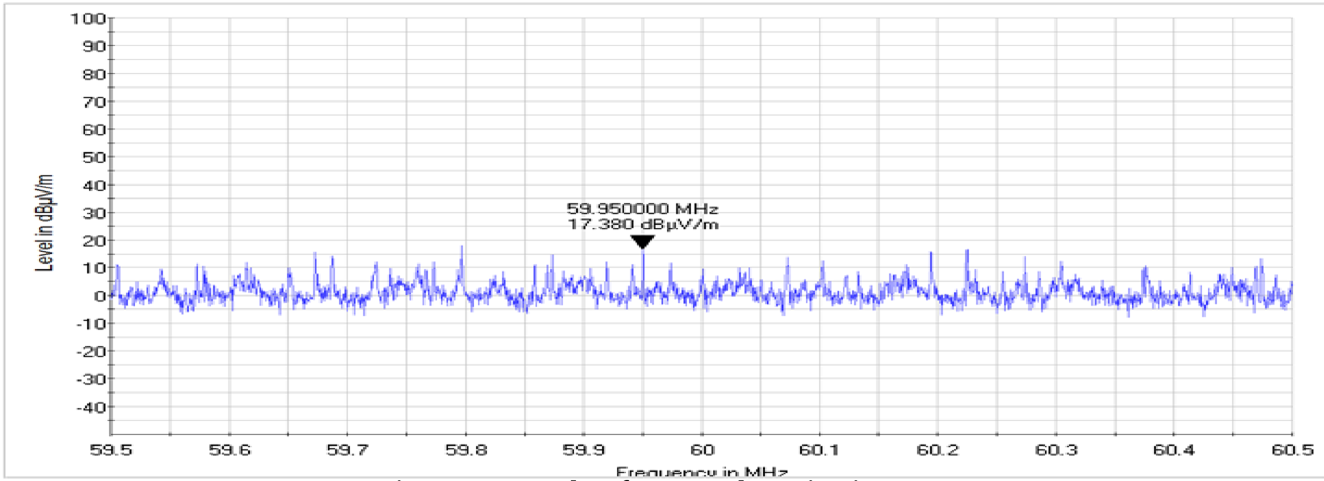

Figure A3. Test data for setup shown in Figure 24.

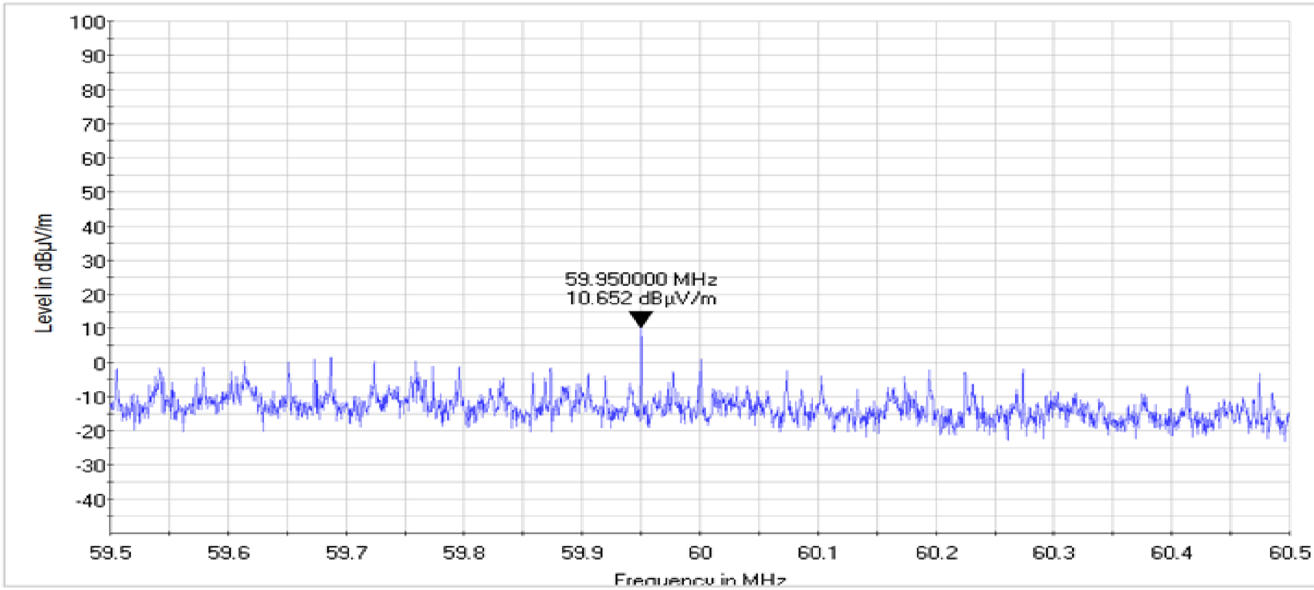

Figure A4. Test data for setup shown in Figure 25.

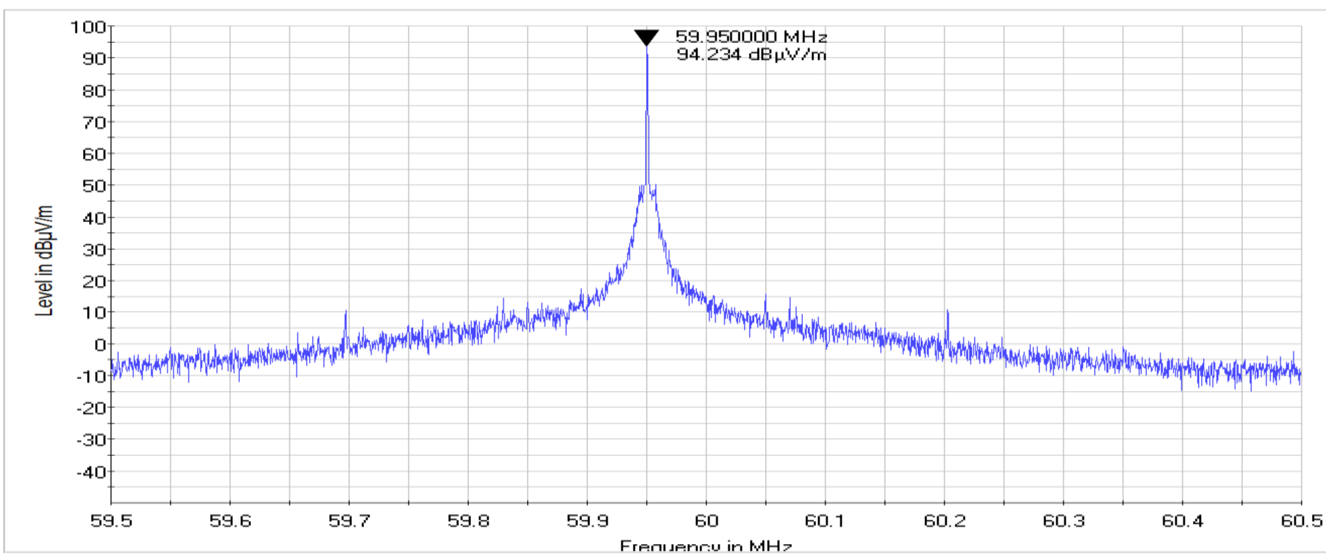

Figure A5. Test data for setup shown in Figure 26.

ACKNOWLEDGEMENTS

This work was performed at the Jet Propulsion Laboratory, California Institute of Technology, under NASA contract. The authors thank fellow Jet Propulsion Laboratory coworkers Todd Krafchak, Subha Comandur, Sasha Eremenko, Jeff Lesovoy, Matt Horner, and Jim Baughman for their guidance on this task. The authors also thank Spira Manufacturing Corporation for their contribution of gaskets and installation guidance.

REFERENCES

[1] *Spira Manufacturing Corporation - Spira-Shield*, www.spira-emi.com/products/sshield.htm.

[2] "Metal Suppliers Online Business Procurement Center." www.metalsuppliersonline.com/.

BIOGRAPHY

Nicholas Keyawa *received a B.S. in Mechanical Engineering from California State University, Northridge (CSUN) in 2011. He has been with JPL for more than 7 years. He was a systems engineer for the MMRTG (Multi-Mission Radioisotope Thermoelectric Generator) on Mars 2020, and worked on developing the technology of next generation thermoelectric generators at JPL. He has also worked on the mechanical design of CSUNSat1, a CubeSat joint project between JPL and CSUN to test a new space rated battery and capacitor. Since 2016, he has been working as a mechanical engineer for the design of the Avionics Vault structure for Europa Clipper.*

Dr. Ali Bahraman *is employed by Bastion Technologies as a member of the JPL EMC Group. As a senior EMC engineer, he has been supporting a number of JPL/NASA projects such as GRACE Follow-ON (GFO), Europa, and EUCLID. He was the Lead EMC engineer on the GFO project. Prior to joining JPL EMC, he was with Raytheon Space and Airborne Systems, El Segundo, CA, where he served as a Senior Principal Engineer and Section Manager in Electromagnetic Environmental Effects Section. He was the Lead EMI Engineer for a number of key programs in Tactical RF systems and Infrared/Visible Sensors for space, notably ASTOR, B-2 RMP, JSF GPS, Glory APS, and VIIRS/NPOESS. Previously, he was with Northrop Grumman Electronics Division, where he was manager of the Radiation Effects and EMC Section. Dr. Bahraman is a Senior Member of the IEEE with a PhD, MS, in Electrical Engineering and BS in Engineering Physics from UC Berkeley.*

William A. Hatch *is the Technical Lead of the Electromagnetic Compatibility Group at the Jet Propulsion Laboratory (JPL) and has worked in that group since 2013. Prior to that, he was a Member of the Technical Staff in the Instruments Division at JPL where he designed, developed, tested and delivered instruments to United States and Foreign customers for near Earth and Deep Space missions. Mr. Hatch has an extensive background in RF and microwave with designs ranging in frequency from DC to over 1 THz. He is an IEEE member and a licensed Electrical Engineer in the State of California.*

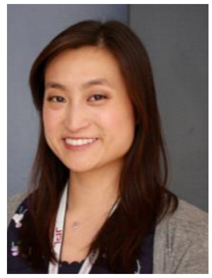

Katherine Dang *has been an Electromagnetic Compatibility Engineer at JPL since 2017 and active in the IEEE EMC Society since 2018. While working in EMC part-time at JPL since 2010, she received a BS in Electrical Engineering from California State Polytechnic University, Pomona and a MS in Electrical Engineering from the University of Southern California. She is currently the deputy lead EMC engineer for the Europa Clipper project, specializing in Magnetic Cleanliness. She has been involved in numerous projects from interplanetary spacecraft to Earth orbiters and technology demonstrations.*

Lou Giersch *has been with JPL for more than 10 years, where he currently works in the Entry, Descent, Landing and Formulation Group. He has previously worked in the deployable structures group at JPL, and he received his PhD in Aeronautics & Astronautics from the University of Washington in Seattle, WA in 2005.*